

学术期刊可以用微信做什么，快来看看！



# 微信自动应答服务平台

—— 微时代 微革命 ——

可全面技术输出



# 微服务

移动互联网时代的营销革命

简单快捷 · 高效互动 · 随时随地 · 广泛传播

微信扫一扫

开启智慧“微服务”



# Q-switched fiber laser operating at 1.5 $\mu\text{m}$ based on $\text{WTe}_2$

Mengli Liu (刘孟丽)<sup>1</sup>, Yuyi Ouyang (欧阳毓一)<sup>1</sup>, Huanran Hou (侯焕然)<sup>1</sup>,  
Wenjun Liu (刘文军)<sup>1,\*</sup>, and Zhiyi Wei (魏志义)<sup>2,\*\*</sup>

<sup>1</sup>State Key Laboratory of Information Photonics and Optical Communications, School of Science, Beijing University of Posts and Telecommunications, Beijing 100876, China

<sup>2</sup>Beijing National Laboratory for Condensed Matter Physics, Institute of Physics, Chinese Academy of Sciences, Beijing 100190, China

\*Corresponding author: [jungliu@bupt.edu.cn](mailto:jungliu@bupt.edu.cn); \*\*corresponding author: [zywei@iphy.ac.cn](mailto:zywei@iphy.ac.cn)

Received October 31, 2018; accepted December 14, 2018; posted online January 23, 2019

Compared with the extensively studied  $\text{MoS}_2$  and  $\text{WS}_2$ ,  $\text{WTe}_2$  owns a smaller bandgap, which is applicable to a near-infrared system in photodetectors, communications, and ultrafast optics. In this work, the  $\text{WTe}_2$  saturable absorber (SA) with the tapered fiber structure is prepared by the magnetron-sputtering technology, which enables the prepared SA to be low in cost and have strong nonlinearity. The modulation depth of the prepared  $\text{WTe}_2$  SA is measured as 31.06%. The Q-switched fiber laser operating at 1.5  $\mu\text{m}$  is successfully investigated by incorporating the proposed SA into the prepared ring cavity. To the best of our knowledge, this is the first attempt of  $\text{WTe}_2$  in the Q-switched fiber laser at 1.5  $\mu\text{m}$ .

OCIS codes: 160.4330, 140.3540, 140.3510.

doi: 10.3788/COL201917.020006.

Pulsed fiber lasers have attracted great attentions owing to the extensive applications in versatile fields, including optical sensing, industrial manufacturing, and optical communication<sup>[1,2]</sup>. Among them, passively Q-switched and mode-locked lasers based on real saturable absorbers (SAs) are preferred because of their merits of compactness, simplicity, and flexibility<sup>[3-12]</sup>. Therefore, high performance SAs are considered to be a hot topic for ultrafast laser research in recent years. At present, the semiconductor SA mirror (SESAM) as the more mature one in commercial laser systems, has received shackles in further development because of its complex process, high price, and limited working band<sup>[13,14]</sup>. The successful strip exfoliation of graphene is a defining point for the discovery and development of stable two-dimensional (2D) layered materials. With the rise of optical nonlinear nanomaterials<sup>[15-17]</sup>, saturable absorption devices are undergoing a revolution, which are characterized by smaller size, easier integration into lasers, cheaper price, wider operating range, and better performance.

Depending on this application demand, some 2D materials are being studied and selected. In particular, transition metal dichalcogenides (TMDs) have become one of the focuses of research. As two of the most widely researched TMDs, molybdenum disulfide ( $\text{MoS}_2$ ) and tungsten disulfide ( $\text{WS}_2$ ) are found to exhibit distinct performance, which is comparable to that of graphene<sup>[18-30]</sup>. But unlike graphene, which owns the zero bandgap, the bandgap value and type of TMDs are closely related to the number of layers. The thickness-dependent band gap and optical properties enable TMDs to have larger development space in photonic devices, including quantum-well modulators, photo detectors, and optical switches.

According to the inherent change rule of TMDs, when the mass of the chalcogen atom increases, for example,

from S to Se to Te, the bandgap decreases synchronously<sup>[31]</sup>. Therefore, compared with the extensively studied  $\text{MoS}_2$  and  $\text{WS}_2$ , tungsten telluride ( $\text{WTe}_2$ ) owns a smaller bandgap. It has been reported that the bandgaps of monolayer and bulk  $\text{WTe}_2$  are 0.7 and 1.18 eV<sup>[32-35]</sup>. This bandgap is applicable to near-infrared systems in photodetectors, communications, and ultrafast optics. Ko *et al.* made some contributions on the investigation of the Q-switched fiber laser operating at 1  $\mu\text{m}$  by employing  $\text{WTe}_2$ <sup>[36]</sup>. However, the Q-switched fiber laser with a longer waveband employed with  $\text{WTe}_2$  has not been implemented yet.

In this work, the  $\text{WTe}_2$  SA with the tapered fiber structure is prepared by the magnetron-sputtering technology (MST). The production process of MST is simple and efficient, which has an advantage in mass production. Compared with chemical vapor deposition, MST has low cost. Besides, the evanescent field interaction between  $\text{WTe}_2$  and light partly increases the damage threshold of  $\text{WTe}_2$  SA. According to previous studies<sup>[33]</sup>, the small waist diameter and long fused zone of the tapered fiber are able to enhance the nonlinearity of SAs. As a result, the prepared SA is low in cost and has strong nonlinearity. The modulation depth of the prepared SA is measured as 31.06%. Moreover, the Q-switched fiber laser operating at 1.5  $\mu\text{m}$  is successfully investigated by means of the prepared SA. The realization of a Q-switched fiber laser proves the broadband absorption property of  $\text{WTe}_2$ , and the impressive performance of the laser further illustrates that  $\text{WTe}_2$  can be a strong candidate for optical switch materials.

In order to improve the nonlinearity of SAs, the selected fibers are tightly controlled in waist diameter and the effective length of the fused zone. The tapered fiber used in the experiment owns the waist diameter of 15  $\mu\text{m}$  and

the fused zone of 1 cm. As mentioned above,  $WTe_2$  is mainly produced by MST. Before production, the  $WTe_2$  target with purity of 99.99% is prepared. Then, both the tapered fiber and  $WTe_2$  target are fixed in the vacuum chamber. The vacuum degree inside the chamber is set to be  $9 \times 10^{-4}$  Pa. In the sputtering process, the Ar ions produced by ionization accelerate to the target under the action of the electric field and bombard the target surface with high energy, which makes the target sputter. In sputtering process, the  $WTe_2$  plasma plume is deposited on the substrate fiber to form a thin film. In order to ensure the uniformity of the particle attachment, the fiber is rotated uniformly at the rotational speed of 20 r/min.

In order to observe the micromorphology of the coating film, the scanning electron microscopy (SEM) as an efficient and low-cost method has been adopted. As shown in Fig. 1(a), the  $WTe_2$  particles on the surface are arranged in close order, which indicates the uniformity of attached particles. From the lateral micro-representation in Fig. 1(b), the thickness of the  $WTe_2$  is measured to be 64 nm.

The Raman spectrum of prepared  $WTe_2$  is shown in Fig. 2(a). Four patterns of vibration that are located at 117.7, 137.5, 175.2, and 219.3  $cm^{-1}$  are observed. According to previous studies, 117.7  $cm^{-1}$  corresponds to mode  $A_1^3$ , 137.5  $cm^{-1}$  corresponds to mode  $A_1^4$ , 175.2  $cm^{-1}$  corresponds to mode  $A_1^7$ , and 219.3  $cm^{-1}$  corresponds to mode  $A_1^9$ , respectively<sup>[37-40]</sup>. As a result, the prepared  $WTe_2$  owns high crystal quality. The nonlinear absorption characteristics of the SA can be measured simply by using the double balance detection method. The home-made laser employed in measurement owns the pulse duration of 600 fs at 1550 nm. By using a variable optical attenuator to adjust the incident power, we get the saturable absorption curve of the  $WTe_2$  SA, as shown in Fig. 2(b). The modulation depth is measured to be 31.06%.

The experimental installation diagram of the proposed Q-switched erbium-doped fiber (EDF) laser employing the taper fiber  $WTe_2$  SA is shown in Fig. 3. The gain medium that the ring cavity adopted is a 0.6-m-long EDF (Liekki 110-4/125). Through a 980/1550 nm wavelength division multiplexer (WDM), the EDF is pumped by a commercial laser diode (LD) that operates at 980 nm. The isolator is inserted into the ring cavity to guarantee unidirectional beam oscillation. Meanwhile, the

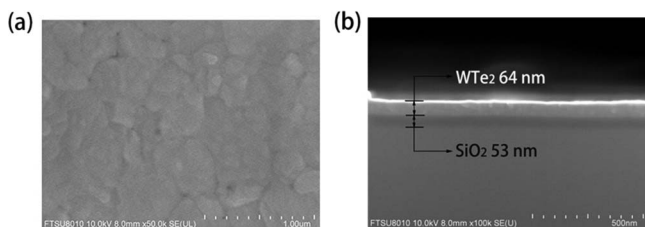


Fig. 1. SEM images of (a) the  $WTe_2$  particles on the surface, and (b) the thickness of the  $WTe_2$ .

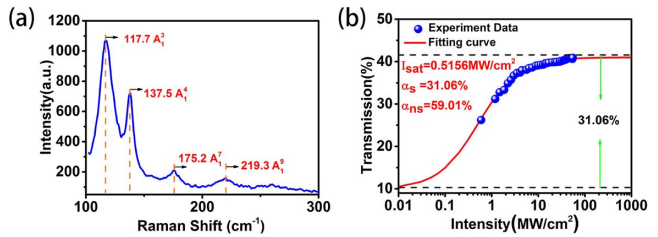


Fig. 2. (a) Raman spectrum of prepared  $WTe_2$ , and (b) the nonlinear absorption characteristics of the  $WTe_2$  SA.

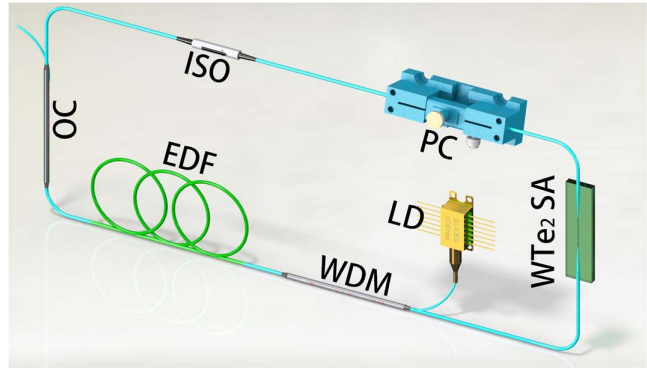


Fig. 3. Experimental installation diagram of the proposed Q-switched EDF laser employing a taper fiber  $WTe_2$  SA.

polarization controller (PC) is included between the isolator and  $WTe_2$  SA to change the polarization state of light and optimize the cavity state. The  $WTe_2$  SA is inserted to be the Q switch. Finally, to extract the real-time laser state of the ring cavity, the 80:20 coupler is included between the EDF and isolator.

When the pump power is set to 212 mW, the stable Q-switched pulses are observed on the oscilloscope. Moreover, this steady operation state is maintained until the laser power increases to 630 mW or even higher. The spectrum of the Q-switched system is shown in Fig. 4(a), which

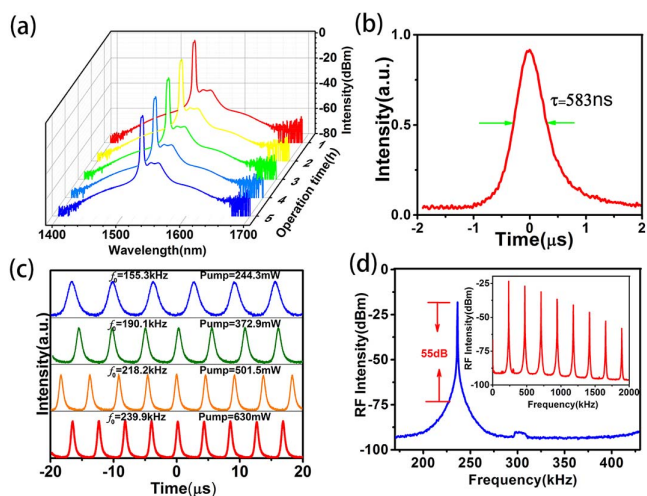


Fig. 4. (a) Spectrum, (b) pulse duration, (c) oscilloscope traces under various pump powers, and (d) RF spectrum.

indicates that the central wavelength is 1531 nm, and the 3 dB bandwidth is measured to be 3.82 nm. The sampled data of 5 h of continuous operation showed no obvious change in spectral shape, indicating that the working state is stable. The central wavelength of a rare-earth-doped fiber laser mainly depends on the cavity conditions, such as cavity propagation loss, active fiber length, and dopant concentration<sup>[41]</sup>, which is the reason for the wavelength shift between working bandwidths of 1531 and 1550 nm. The corresponding pulse duration is 583 ns when pump power is 630 mW, as shown in Fig. 4(b). Meanwhile, the oscilloscope traces under various pump powers are summarized in Fig. 4(c). Along with the strengthening of pump power, the repetition rate increases synchronously. Fig. 4(d) summarizes the radio-frequency (RF) spectra with different ranges. The signal-to-noise ratio (SNR) is measured to be 55 dB, which indicates that the system is relatively stable. Moreover, the fundamental frequency and frequency multiplication show a uniform attenuation trend in the illustrations.

Subsequently, we have systematically generalized the laser performance and the changing process in Fig. 5. Along with the strengthening of pump power, the repetition rate increases synchronously, while the pulse duration decreases, as in Fig. 5(a). The sharp decline of pulse

duration is considered to result from the partially bleached effect of the SA, and the part that tends to be stable is considered to be the material that is nearly saturated. The variation tendencies of pulse energy and output power are shown in Fig. 5(b) at the same time. We can see that their upward trend is maintained, which indicates that the material works under the threshold at this point, and the optimal output can be obtained by optimizing the cavity conditions and increasing the pump power. The maximum average output power and pulse energy we get are  $\sim 14.07$  mW and  $\sim 58.625$  nJ.

In order to highlight the characteristics of the system, a more comprehensive performance comparison is provided. Table 1 shows the performance summary of the passively  $Q$ -switched laser system employing different SAs. As the same TMD member, the modulation depth of  $WTe_2$  is higher. We attribute the high modulation depth to the SA's tapered fiber structure. The small waist diameter and long fused zone of the tapered fiber are able to enhance the nonlinearity of the SA. Meanwhile, the insertion loss of the  $WTe_2$  SA increases to 3.8 dB due to the tapered fiber structure, which also causes the high threshold of the  $Q$ -switching system. To the best of our knowledge, this is the first successful application of a  $WTe_2$  SA in a  $Q$ -switched fiber laser at 1.5  $\mu\text{m}$ . Moreover, the pulse duration achieved in our experiment is the shortest in the table, which indicates that  $WTe_2$  has strong potential and better development space in the field of ultrafast lasers. Besides, both the SNR and output power of the  $Q$ -switched system are impressive. The discussion above indicates that the tapered fiber  $WTe_2$  is a better candidate for SA in passively  $Q$ -switched lasers.

In conclusion, the  $WTe_2$  SAs prepared by MST are successfully applied in a  $Q$ -switched fiber laser at 1.5  $\mu\text{m}$ . The tapered fiber structure of the  $WTe_2$  SA enables it to have strong nonlinearity. The modulation depth of the prepared  $WTe_2$  SA is measured as 31.06%. At 1531 nm, the stable

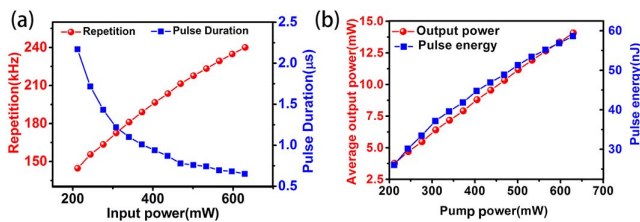


Fig. 5. (a) Trend curves of pulse duration and repetition rate with power variation, and (b) trend curves of average output power and pulse energy with power variation.

**Table 1.** Performance Summary of Passively  $Q$ -switched Laser Systems Employing Different SAs

Materials	Modulation Depth (%)	Wavelength (nm)	$Q$ -switching Threshold (mW)	Repetition Rate (kHz)	Pulse Duration ( $\mu\text{s}$ )	Power (mW)	SNR (dB)	Energy (nJ)	Ref.
Graphene	1.5	0.02/1539.6	8.3	10.36–41.8	3.89	3.38	30	28.7	[42]
$Bi_2Se_3$	30	0.2/1543.2	45	2.6–12	9.5	<0.05	40	4	[43]
$Bi_2Te_3$	10.8	2/1562.9	67	7.5–42.8	2.81	0.55	–	12.7	[44]
BP	18.55	0.2/1562.87	50	6.983–15.78	13.2	<1.5	45	94.3	[45]
$WS_2$	0.99	–/1560.7	40	27.2–84.8	1.73	$\sim 0.3$	43.7	$\sim 11$	[46]
$MoS_2$	1.6	0.16/1565	15.5	6.5–27	7.5	1.7	54.5	63.2	[26]
$WSe_2$	3.5	–/1560	140	4.5–49.6	3.9	1.23	46.7	17	[47]
$MoSe_2$	4.7	–/1566	–	26.5–35.4	5.65	24.5	–	825	[48]
$WTe_2$	31.06	3.82/1531	212	144.7–240	0.583	14.07	55	58.625	This work

laser pulses with the pulse duration of 583 ns are obtained, and the corresponding 3 dB bandwidth is measured to be 3.82 nm. The SNR up to 55 dB confirms the stability of the system. The maximum output power and pulse energy are measured as  $\sim 14.07$  mW and  $\sim 58.625$  nJ. To the best of our knowledge, this is the first successful application of a WTe<sub>2</sub> SA in a Q-switched fiber laser at 1.5  $\mu\text{m}$ . Moreover, the short pulse duration of 583 ns is impressive. Our results not only confirm the broadband absorption properties of WTe<sub>2</sub>, but also make a prospective exploration and pave the way for WTe<sub>2</sub> in the field of ultrafast lasers.

## References

- U. Keller, *Nature* **424**, 831 (2003).
- B. Oktem, C. Ülgüdüir, and F. Ö. Ilday, *Nat. Photon.* **4**, 307 (2010).
- Z. Sun, A. Martinez, and F. Wang, *Nat. Photon.* **10**, 227 (2016).
- Q. L. Bao, H. Zhang, Y. Wang, Z. H. Ni, Y. L. Yan, Z. X. Shen, K. P. Loh, and D. Y. Tang, *Adv. Funct. Mater.* **19**, 3077 (2009).
- C. Zhang, J. Liu, X. W. Fan, Q. Q. Peng, X. S. Guo, D. P. Jiang, X. B. Qian, and L. B. Su, *Opt. Laser Technol.* **103**, 89 (2018).
- J. Liu, Y. G. Wang, Z. S. Qu, and X. W. Fan, *Opt. Laser Technol.* **44**, 960 (2012).
- M. X. Lin, Q. Q. Peng, W. Hou, X. W. Fan, and J. Liu, *Opt. Laser Technol.* **109**, 90 (2019).
- K. Wu, B. H. Chen, X. Y. Zhang, S. F. Zhang, C. S. Guo, C. Li, P. S. Xiao, J. Wang, L. J. Zhou, W. W. Zou, and J. P. Chen, *Opt. Commun.* **406**, 214 (2018).
- F. Zhang, Y. J. Wu, J. Liu, S. Y. Pang, F. K. Ma, D. P. Jiang, Q. H. Wu, and L. B. Su, *Opt. Laser Technol.* **100**, 294 (2018).
- H. T. Zhu, J. Liu, S. Z. Jiang, S. C. Xu, L. B. Su, D. P. Jiang, X. B. Qian, and J. Xu, *Opt. Laser Technol.* **75**, 83 (2015).
- Y. J. Wu, C. Zhang, J. J. Liu, H. N. Zhang, J. M. Yang, and J. Liu, *Opt. Laser Technol.* **97**, 268 (2017).
- C. Li, M. W. Fan, J. Liu, L. B. Su, D. P. Jiang, X. B. Qian, and X. Jun, *Opt. Laser Technol.* **69**, 140 (2015).
- W. Cai, Q. Q. Peng, W. Hou, J. Liu, and Y. G. Wang, *Opt. Laser Technol.* **58**, 194 (2014).
- O. Okhotnikov, A. Grudinin, and M. Pessa, *New J. Phys.* **6**, 177 (2004).
- S. C. Dhanabalan, J. S. Ponraj, H. Zhang, and Q. Bao, *Nanoscale* **8**, 6410 (2016).
- Y. L. Ying, Y. F. Yang, W. Ying, and X. S. Peng, *Nanotechnology* **27**, 332001 (2016).
- J. Ma, S. B. Lu, Z. N. Guo, X. D. Xu, H. Zhang, D. Y. Tang, and D. Y. Fan, *Opt. Express* **23**, 22643 (2015).
- J. T. Wang, Z. K. Jiang, H. Chen, J. R. Li, J. D. Yin, J. Z. Wang, T. C. He, P. G. Yan, and S. C. Ruan, *Photon. Res.* **6**, 535 (2018).
- W. Y. Li, Y. Y. OuYang, G. L. Ma, M. L. Liu, and W. J. Liu, *Laser Phys.* **28**, 055104 (2018).
- M. Zhang, R. C. T. Howe, R. I. Woodward, E. J. R. Kelleher, F. Torrisi, G. H. Hu, S. V. Popov, J. R. Taylor, and T. Hasan, *Nano Res.* **8**, 1522 (2015).
- J. T. Wang, H. Chen, Z. K. Jiang, J. D. Yin, J. Z. Wang, M. Zhang, T. C. He, J. Z. Li, P. G. Yan, and S. C. Ruan, *Opt. Lett.* **43**, 1998 (2018).
- W. J. Liu, M. L. Liu, H. N. Han, S. B. Fang, H. Teng, M. Lei, and Z. Y. Wei, *Photon. Res.* **6**, C15 (2018).
- P. G. Yan, Z. K. Jiang, H. Chen, J. D. Yin, J. T. Lai, J. Z. Wang, T. C. He, and J. B. Yang, *Opt. Lett.* **43**, 4417 (2018).
- K. Wu, C. S. Guo, H. Wang, X. Y. Zhang, J. Wang, and J. P. Chen, *Opt. Express* **25**, 17639 (2017).
- W. J. Liu, M. L. Liu, J. D. Yin, H. Chen, W. Lu, S. B. Fang, H. Teng, M. Lei, P. G. Yan, and Z. Y. Wei, *Nanoscale* **10**, 7971 (2018).
- Z. Q. Luo, Y. Z. Huang, M. Zhong, Y. G. Li, J. Y. Wu, B. Xu, H. Y. Xu, Z. P. Cai, J. Peng, and J. Weng, *J. Lightwave Technol.* **32**, 4679 (2014).
- W. J. Liu, M. L. Liu, Y. Y. OuYang, H. Hou, M. Lei, and Z. Y. Wei, *Nanotechnology* **29**, 394002 (2018).
- M. L. Liu, Y. Y. OuYang, H. R. Hou, M. Lei, W. J. Liu, and Z. Y. Wei, *Chin. Phys. B* **27**, 084211 (2018).
- G. Z. Wang, S. F. Zhang, X. Y. Zhang, L. Zhang, Y. Cheng, D. Fox, H. Z. Zhang, J. N. Coleman, W. J. Blau, and J. Wang, *Photon. Res.* **3**, A51 (2015).
- H. D. Xia, H. P. Li, C. Y. Lan, C. Li, X. X. Zhang, S. J. Zhang, and Y. Liu, *Opt. Express* **22**, 17341 (2014).
- D. Mao, B. B. Du, D. X. Yang, S. L. Zhang, Y. D. Wang, W. D. Zhang, X. Y. She, H. C. Cheng, H. B. Zeng, and J. L. Zhao, *Small* **12**, 1489 (2016).
- A. Kumar and P. K. Ahluwalia, *Eur. Phys. J. B* **85**, 186 (2012).
- C. H. Lee, E. C. Silva, L. Calderin, M. A. Nguyen, M. J. Hollander, B. Bersch, T. E. Mallouk, and J. A. Robinson, *Sci. Rep.* **5**, 10013 (2015).
- B. Ghosh, A. Gupta, and B. Bishnoi, *J. Semicond.* **35**, 113002 (2014).
- W. J. Liu, L. H. Pang, H. N. Han, K. Bi, M. Lei, and Z. Y. Wei, *Nanoscale* **9**, 5806 (2017).
- S. Ko, J. Lee, and J. H. Lee, *Chin. Opt. Lett.* **16**, 020017 (2018).
- Y. Kim, Y. I. Jhon, J. Park, J. H. Kim, S. Lee, and Y. M. Jhon, *Nanoscale* **8**, 2309 (2016).
- Q. S. Wang, J. Li, J. Besbas, C. H. Hsu, K. M. Cai, L. Yang, S. Cheng, Y. Wu, W. F. Zhang, K. Y. Wang, T. Chang, H. Lin, H. X. Chang, and H. Yang, *Adv. Sci.* **5**, 1700912 (2018).
- J. Koo, Y. I. Jhon, J. Park, J. Lee, Y. M. Jhon, and J. H. Lee, *Adv. Funct. Mater.* **26**, 7454 (2016).
- L. A. Walsh, R. Yue, Q. X. Wang, A. T. Barton, R. Addou, C. M. Smyth, H. Zhu, J. Kim, L. Colombo, M. J. Kim, R. M. Wallace, and C. L. Hinkle, *2D Mater.* **4**, 025044 (2017).
- P. Franco, M. Midrio, A. Tozzato, M. Romagnoli, and F. Fontana, *J. Opt. Soc. Am. B* **11**, 1090 (1994).
- J. Wang, Z. Luo, M. Zhou, C. Ye, H. Fu, Z. Cai, H. Cheng, H. Xu, and W. Qi, *IEEE Photon. J.* **4**, 1295 (2012).
- S. Q. Chen, Y. Chen, M. Wu, Y. Li, C. J. Zhao, and S. C. Wen, *IEEE Photon. Tech. Lett.* **26**, 987 (2014).
- J. Koo, J. Lee, C. Chi, and J. H. Lee, *J. Opt. Soc. Am. B* **31**, 2157 (2014).
- Y. Chen, G. B. Jiang, S. Q. Chen, Z. N. Guo, X. F. Yu, C. J. Zhao, H. Zhang, Q. L. Bao, S. C. Wen, D. Y. Tang, and D. Y. Fan, *Opt. Express* **23**, 12823 (2015).
- H. Ahmad, N. E. Ruslan, M. A. Ismail, S. A. Reduan, C. S. J. Lee, S. Sathiyam, S. Sivabalan, and S. W. Harun, *Appl. Opt.* **55**, 1001 (2016).
- B. Chen, C. Guo, K. Wu, J. Chen, X. Zhang, and J. Wang, *Opt. Eng.* **55**, 081306 (2016).
- R. I. Woodward, R. C. T. Howe, T. H. Runcorn, G. Hu, F. Torrisi, E. J. R. Kelleher, and T. Hasan, *Opt. Express* **23**, 20051 (2015).